Preprints.org

Article

Pyrolysis of Solid Recovered Fuel using Fixed and Fluidized Bed Reactor

Myeongjong Lee , Hyeongtak Ko , Seacheon Oh [*]

Article

Pyrolysis of Solid Recovered Fuel using Fixed and Fluidized Bed Reactor

Myeongjong Lee [1], Hyeongtak Ko [1] and Seacheon Oh [1,*]

[1] Department of Environmental Engineering, Kongju National University, 1223-24 Cheonan-Daero, Seobuk, Cheonan 31080, Chungcheongnam-do, Korea ; dlaudwhd77@naver.com

[*] Correspondence: ohsecl@kongju.ac.kr; Tel.: +82-41-521-9423

Abstract: Currently, most plastic waste stems from packaging materials, with a large proportion of this waste either discarded or used to derive fuel. Accordingly, there is growing interest in the use of pyrolysis in the context of chemically recycling non-recyclable (i.e., via mechanical means) plastic waste into petrochemical feedstock. The aim of this study is to use kinetic analyses to elucidate the pyrolytic properties of solid recovered fuel (SRF) produced using two types of reactors, namely, fixed bed and fluidized bed reactors. From the kinetic analysis, the activation energy corresponding to the rate of pyrolysis reaction conversion was obtained. In conclusion, we found that the pyrolysis occurs more vigorously in fluidized bed reactors compared to fixed bed reactors.

Keywords: pyrolysis; solid recovered fuel; fixed bed reactor; fluidized bed reactor; kinetic analysis

1. Introduction

The past few decades have seen a continuous increase in the production and demand for plastics. This trend can be attributed not only to the diverse physiochemical properties of plastics, which allow for their wide applicability, but also to their low cost. However, this surge in plastic usage has not been without consequences, with one being the increase in plastic waste. For example, it has been reported that plastic waste constitutes more than 50% of waste produced by the average household [1]. Therefore, in light of the long-term persistence of plastic in the environment, recycling plastic waste has been highlighted as a crucial step in the context of the large-scale establishment of a circular economy to attain carbon neutrality [2]. However, approximately 40% of all plastic waste is generated from packaging materials, whereas approximately 60% of this waste is neither recycled nor reused, instead, it is channeled toward energy recovery or disposed of [3]. Unlike biomass, these waste plastics do not biodegrade, instead, if unaided, they undergo a decomposition that can take more than four centuries to reach its conclusion. In addition, this decomposition does not occur uneventfully, as it has been linked to the accumulation of wide-reaching pollutants in landfills [4,5]. Plastics mainly consist of LDPE (Low-density Polyethylene), HDPE (Low-density Polyethylene), PP (Polypropylene), PS (Polystyrene), PET (Polyethylene Terephthalate), and PVC (Polyvinyl Chloride). Among these constituents, PE, PP, and PS make up 50-70% of most plastics [6,7]. To facilitate the optimal recycling of plastic waste, it first has to be sorted based on its physiochemical make. However, considering the mixed nature of plastic waste, the processes currently used to sort it are plagued by numerous limitations; this is a serious issue, especially considering the fact that the efficiency of mechanical recycling for material reuse is highly dependent on the effectiveness of the sorting processes used to scan for contaminants [8]. However, in a situation in which the sorting or separation of intrinsically heterogeneous plastic waste is not optimal, another layer of inefficiency is introduced in the already-disorganized, wasteful plastic recycling industry. Additionally, since mechanical recycling typically tends to be accompanied by the degradation of plastic, alternative methods to conventional mechanical recycling must be considered, especially in the context of ensuring the sustainable use of plastics in a circular economy [9]. Plastics, as materials derived from petrochemical feedstocks, are a mosaic of hydrocarbon compounds; these properties manifest themselves in plastics containing an inherent wealth of recoverable chemical energy [6,10]. Thus,
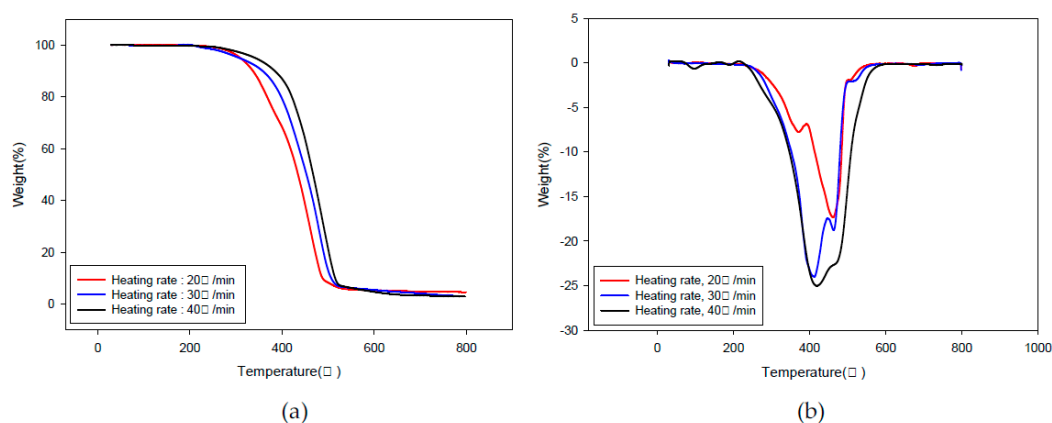
chemical recycling through pyrolysis is gaining attention as one of the options for recycling plastic waste into petrochemical feedstocks. Pyrolysis is a reaction that decomposes high molecular weight compounds with long-chain structures into low molecular weight compounds; this process occurs via heat application in an anaerobic environment, with its yields being char, oil, and gaseous substances [11]. Pyrolysis addresses a major drawback of traditional mechanical recycling—the inability to allow for continuous recycling—by offering the opportunity to recover otherwise non-recyclable waste plastics [12]. It has been shown that the calorific value of pyrolysis-derived oil produced from plastic waste is comparable to conventional diesel fuel, allowing it to serve as a robust replacement. Moreover, the materials generated post-pyrolysis can be reused in existing petrochemical processes, making them an excellent alternative in the energy market [13-18].

In South Korea, a specific recycling rate is mandated for plastic packaging materials by the Extended Producer Responsibility (EPR) system. Accordingly, this waste is either mechanically recycled or used as solid recovered fuel (SRF). Therefore, this study aimed to investigate the pyrolytic properties of SRF produced from plastic waste, specifically plastic that was once used as packaging. To achieve this aim, we used both batch fixed bed and continuous fluidized bed reactors. We then comprehensively compared the SRF produced through the two types of reactors, with the comparison largely centered on its yield and pyrolytic properties. Additionally, using kinetic analyses, we determined the activation energy required for the pyrolysis of SRF in the context of the abovementioned reactors.
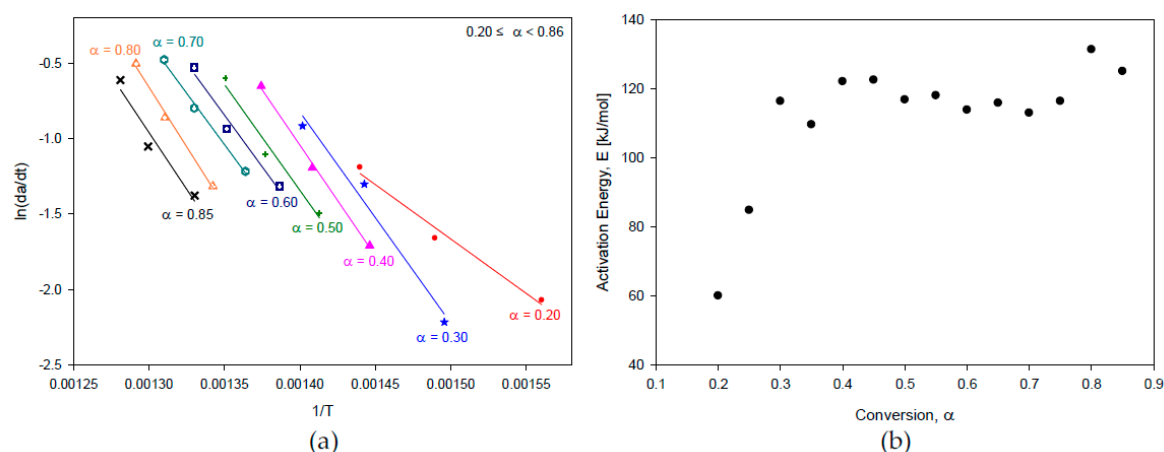
2. Results and Discussion

2.1. Kinetic Analysis

Figure 1 shows the TG (thermogravimetric) and DTG (derivative thermogravimetric) curves, illustrating the heating rates under a nitrogen atmosphere for kinetic analysis of the pyrolysis of the SRF. The TG curve in Figure 1a shows that the decomposition temperature rises as the heating rate increases, likely due to thermal transfer lag caused by the increased heating rate. Additionally, Figure 1b's DTG curve shows more than two peaks, confirming that the SRF used in this study is a heterogeneous mixture of different plastics. The SRF used in this study is primarily made from plastic packaging waste composed of PP and PE. Generally, PP begins to undergo pyrolysis at 400 ℃, whereas PE does so at a higher temperature [19, 20]. Therefore, the peak at ~400 ℃ in the DTG curve is likely due to the pyrolysis of PP, and the subsequent peak (between 450–500 ℃) is likely due to PE. The activation energies for each conversion rate were determined by applying the differential method described in Equation (2), and these are presented in Figure 2. Figure 2b shows that the activation energy increases (from 59.9 to 116.3 kJ/mol) as the conversion rate rises up to 0.35, after which it remains fairly constant (between 112.9 and 131.3 kJ/mol). This trend can be attributed to the SRF sample used in this study being a composite of plastics mostly made of PE and PP; the initial conversion rates are primarily due to PP, while subsequent rates are influenced by the pyrolysis of PE.
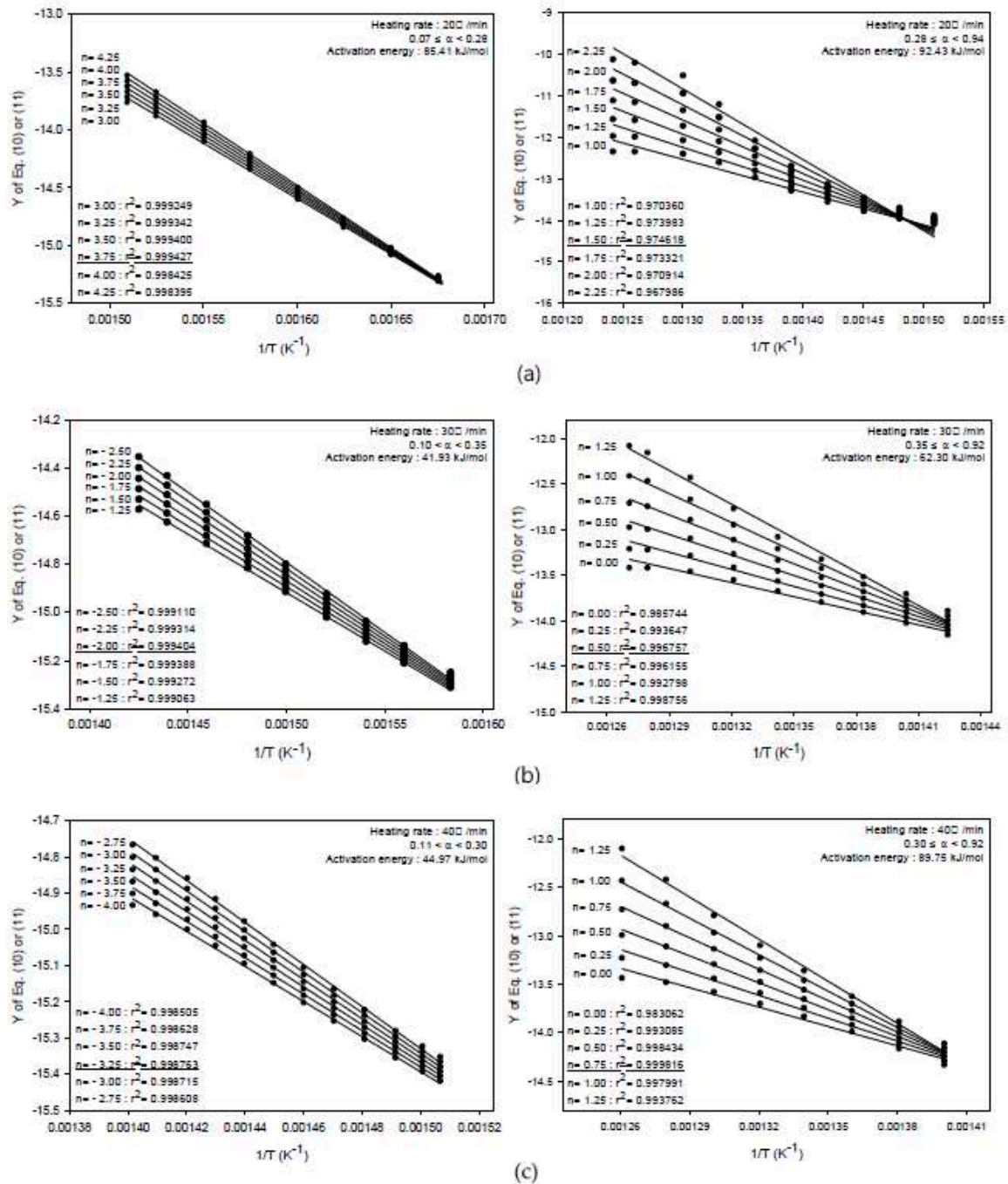

Figure 1. TG (a) and DTG (b) curves of SRF across various heating rates in pure nitrogen.

Figure 2. Application of differential method (a) and activation energies (b) over a range of conversion.

Figure 3 shows the outputs of the integral methods, encapsulated in Equations (10) and (11), to obtain activation energies at various heating rates. The range of conversion rates for obtaining activation energy at each heating rate in Figure 3 was set based on the peaks observed in the DTG analysis in Figure 1b, and was applied in two stages. Figure 3 shows that when using the integral method, the activation energies appear to be lower than those elucidated via the differential method (Figure 2). However, the tendency for the activation energy to be lower in the initial stages of pyrolytic conversion remained consistent with the results obtained using the differential method.

Figure 3. Activation energies at various heating rates of 20°C/min (a), 30°C/min (c) and 40°C/min (c), as determined using the integral method.

Table 1 shows a comparison of the activation energies for the pyrolysis reaction of SRF obtained from the different kinetic analysis methods we applied. We found that in the context of the pyrolysis reactions of PP and PE, the activation energy for the pyrolysis of PP appears to be lower than that of PE [21]. Therefore, although there were differences in the activation energy values based on the kinetic analysis methods, PP was the first to decompose, followed by PE in subsequent stages. This confirmed the validity of the kinetic analysis method used, as the activation energy for the initial pyrolysis of PP is lower than that for the later stages of PE decomposition.

Table 1. Activation energy of pyrolysis of SRF used in this work.

Differential Method		Integral Method		
Conversion (α)	Activation Energy (kJ/mol)	Heating Rate	Conversion (α)	Activation Energy (kJ/mol)
0.20≤a<0.40	59.94 ~ 116.32	20°C/min	0.07≤a<0.28	85.41
			0.28≤a<0.94	92.43
		30°C/min	0.10≤a<0.35	41.93
			0.35≤a<0.92	62.30
0.40≤a<0.85	112.47 ~ 131.32	40°C/min	0.11≤a<0.30	44.97
			0.30≤a<0.92	89.75

2.2. Product Analysis

2.2.1. Fixed Bed Reactor

Figure 4 shows the changes in yield for each product based on the pyrolysis reaction temperature when SRF is pyrolyzed using a fixed bed reactor. As the pyrolysis reaction temperature increases, the yield of liquid products such as heavy oil and light oil decreases (Figure 4). This is likely because the gasification reactions become more active, increasing the yield of gaseous products. Additionally, while the solid residue showed a slight decrease in yield when the reaction temperature exceeded 550℃, the temperature-dependent changes it underwent were minimal.
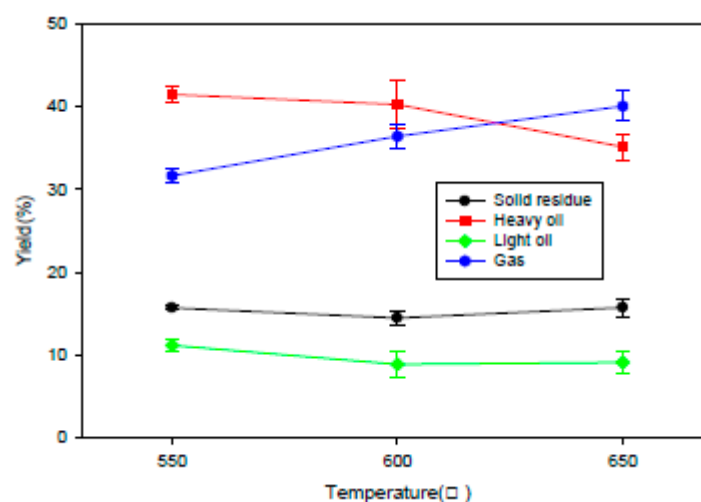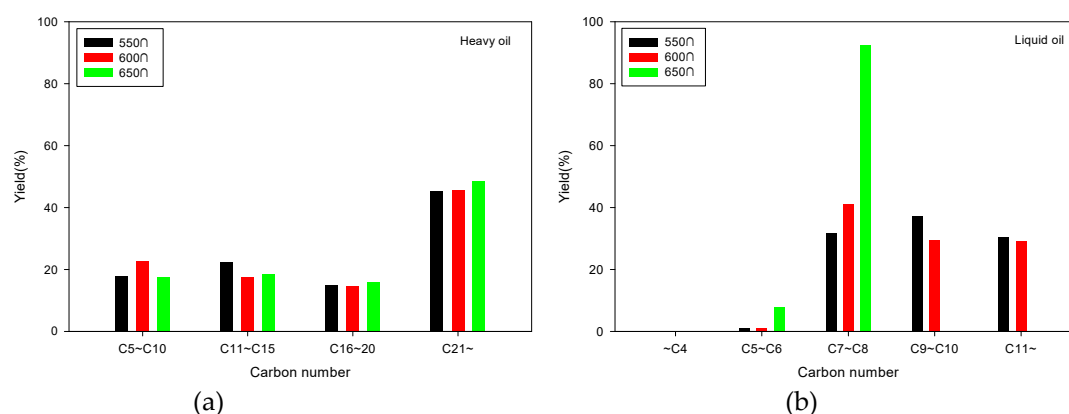

Figure 4. Product yields of SRF pyrolysis using fixed bed reactor across different temperatures.
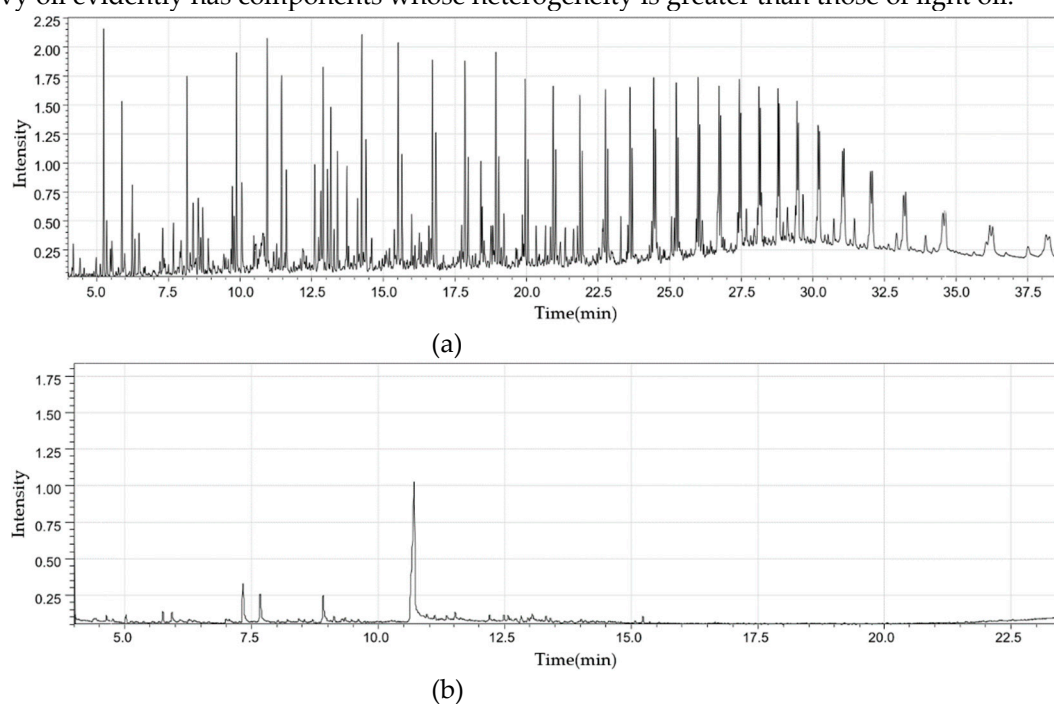
Figure 5 displays the characteristics of the liquid products' carbon number obtained from GC-MS analysis of SRF pyrolysis using a fixed bed reactor. Figure 5 shows that heavy oil mostly consists of components with carbon numbers greater than C21, culminating in the impact of the pyrolysis reaction temperature on its composition being minimal. Heavy oil also contains components in the C5–C10 range, suggesting that a more refined condensation process could potentially increase the yield of light oil. On the other hand, light oil mostly consists of components in the C7 –C8 range. As the reaction temperature increased, there was a noticeable increase in lower molecular weight components, especially at 650℃, culminating in all the components having carbon numbers of C8 or less. This is likely because the pyrolysis reactions become more intense as the reaction temperature increases. However, temperatures that are too high can yield liquid products due to the corresponding increase in the yield of gaseous products. Therefore, selecting the optimal pyrolysis

reaction temperature for SRF should entail considering the yield changes for each product in Figure 4.

(a)   (b)

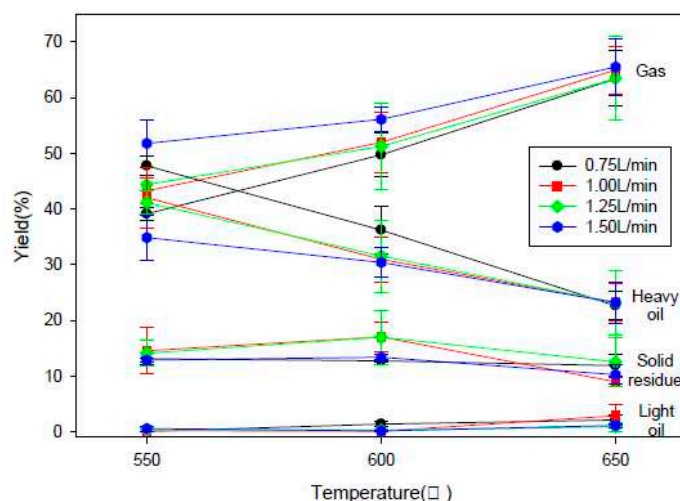**Figure 5.** Compounds according to the carbon number of heavy (a) and light oil (b) obtained from fixed bed reactor.

Figure 6 shows the gas chromatogram for liquid products at a reaction temperature of 600℃. Heavy oil evidently has components whose heterogeneity is greater than those of light oil.

(a)

(b)

Figure 6. Gas chromatogram of heavy (a) and light oil (b) obtained from a fixed bed reactor at a reaction temperature of 600℃.

2.2.2. Fluidized Bed Reactor

Figure 7 shows the changes in yield for each product based on the pyrolysis reaction temperature and the fluidized gas flow rate when SRF is pyrolyzed using a fluidized bed reactor.
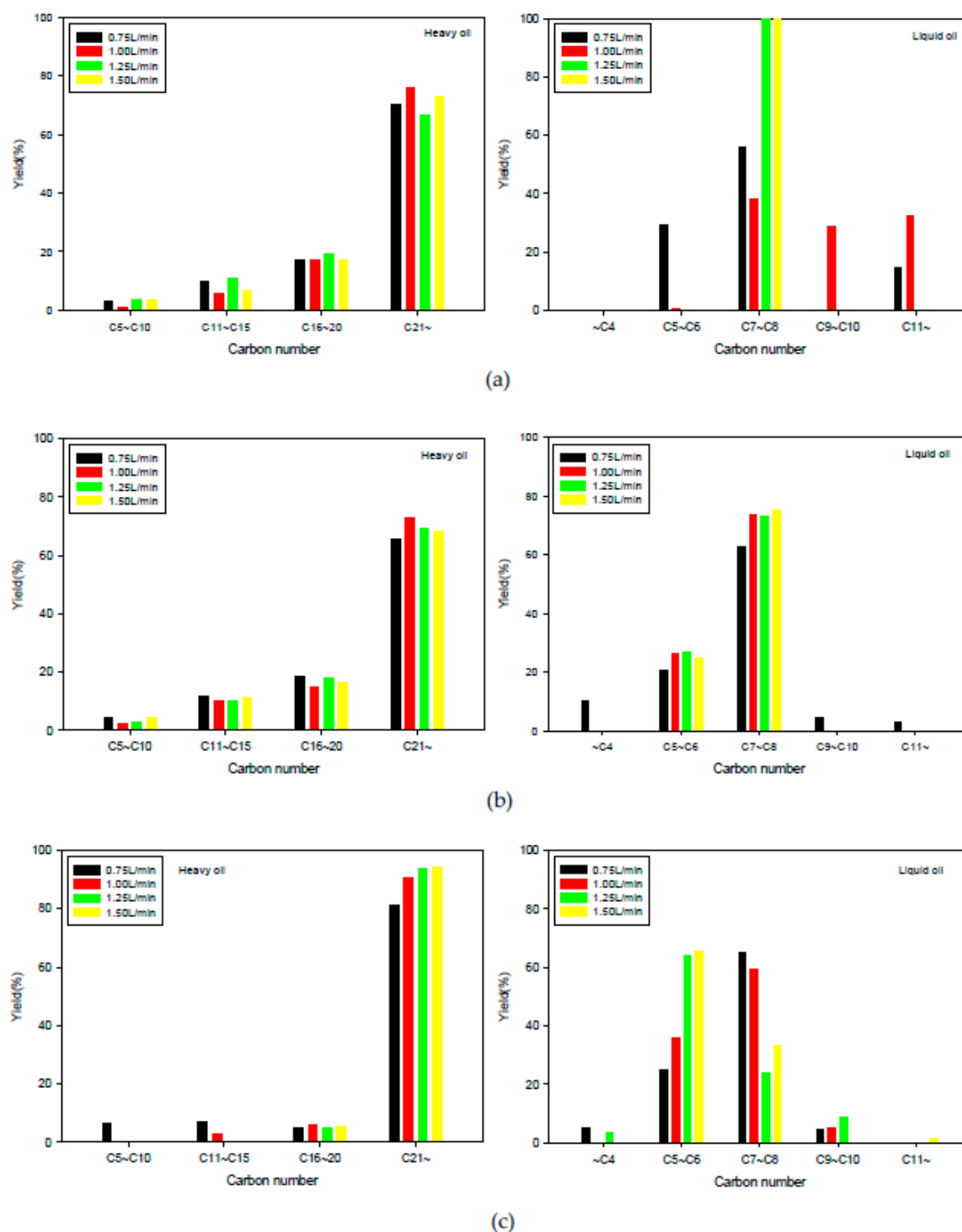
Figure 7. Product yields of SRF pyrolysis using fluidized bed reactor according to temperatures and fluidized gas flow rate.

Figure 7 shows that compared to ouputs obtained via a fixed bed reactor, as the reaction temperature increases, the yield of gaseous products significantly increases, substantially decreasing the yield of heavy oil. Fluidized bed reactions are known to enhance material and heat transfer compared to fixed bed reactions in the pyrolysis of waste plastics [22]. Therefore, we believe that the increase in material and heat transfer due to the fluidized gas results in fluidized bed reactors facilitating a more thorough decomposition of SRF. This trend is further confirmed by the increase in gaseous products as the fluidized velocity increases. Additionally, compared to the fixed bed reactor, the fluidized reactor produced a greater yield of gaseous products; this is because fluidized reactors inherently facilitate a decomposition (i.e., into smaller molecular weight components) that is more intensive than that seen in fixed bed reactors. On the other hand, in the case of light oil, while a slight decrease is observed as the reaction temperature increases in fixed bed reactions, an increase is noted in fluidized bed reactions. Therefore, as previously mentioned, we confirmed that SRF decomposes into lower molecular weight components more readily in fluidized bed reactions compared to fixed bed reactions. For the solid residues, temperature-driven changes were nearly negligible, similar to those in fixed bed reactions.
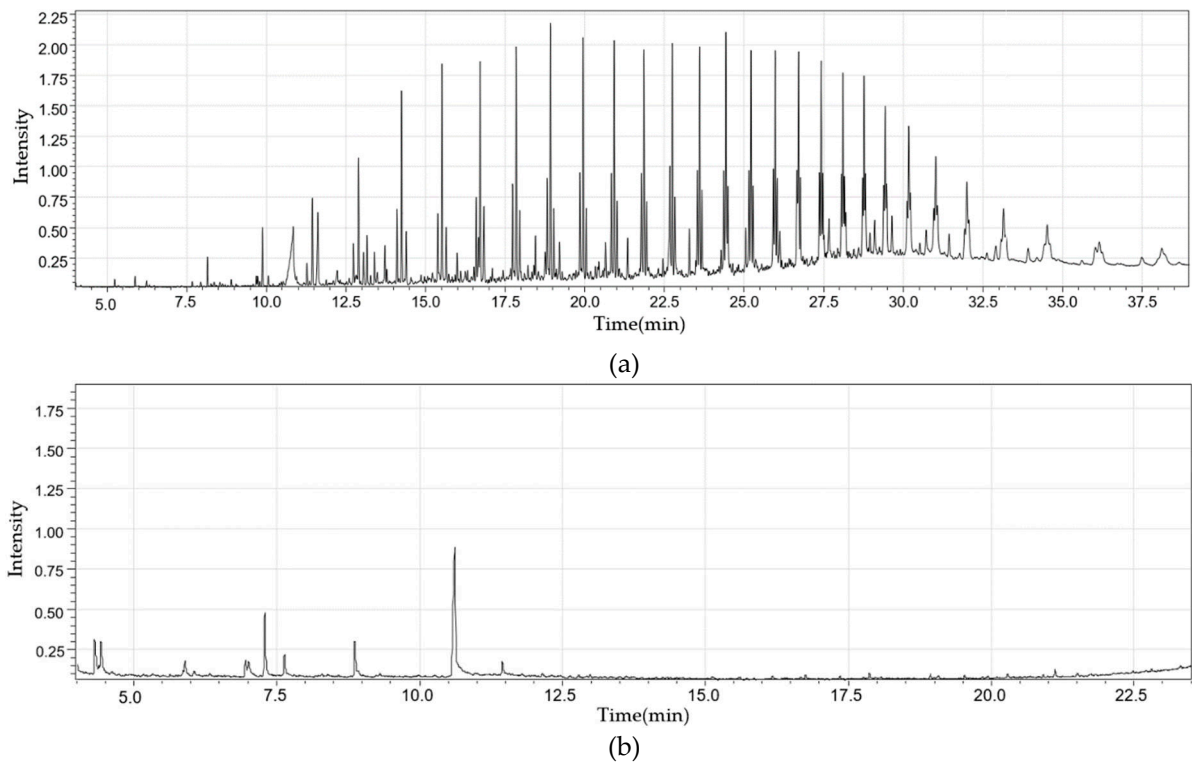
Figure 8 shows the characteristics of the liquid products' carbon number obtained from GC-MS analysis of SRF pyrolysis using a fluidized bed reactor. Figure 8 suggests that, similar to fixed bed reactions, components with a carbon number of C21 and above are most prevalent in heavy oil. However, the proportion of these high-carbon components is higher in fluidized bed reactions, especially at 650℃, where they are produced in substantial amounts. This could be due to the pyrolysis of SRF in fluidized bed reactors, progressing more rapidly than in fixed bed reactors. As a result, the hydrogen content in the liquid products decreases, leading to the formation of oils with higher molecular weights, and higher C/H ratios. Also, in the case of light oil, components ranging from C7–C8 predominate, similar to fixed bed reactions. We observed that lower molecular weight components increase as the reaction temperature and fluidized gas velocity increase.

Figure 8. Compounds according to the carbon number of heavy and light oil obtained from fluidized bed reactor at reaction temperatures of 550 (a), 600 (b), and 650°C (c).

Figure 9 exemplifies the gas chromatograms of heavy and light oil obtained at a reaction temperature of 600°C and a fluidized gas flow rate of 1.0L/min. This trend shows that the composition of heavy oil is more diverse than that of light oil, consistent with the outputs of the fixed bed reactor.

Figure 9. Gas chromatogram of heavy (a) and light oil (b) obtained from a fluidized bed reactor at a reaction temperature of 600°C and a gas flow rate of 1.0L/min.

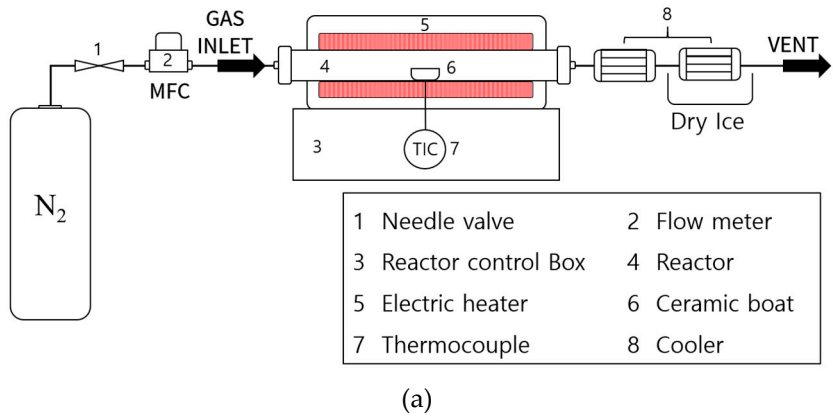## 3. Materials and Methods

3.1. Materials

In this study, SRF produced mainly from packaging waste consisting of PP and PE was used as the pyrolysis feedstock. The characteristics of the SRF samples used in this study are shown in Table 2. The composition of the resultant output was then analyzed using an elemental analyzer (EA) (Flash 2000, UK). These results are tabulated in Table 2. Specifically, Table 2 shows that the resultant material primarily consists of carbon and hydrogen, with nitrogen and oxygen attributed to the presence of trace amounts of ABS (acrylonitrile butadiene styrene) and PET (polyethylene terephthalate) in the plastic waste. The fact that most of the packaging used is made of plastic is reflected in the high amount of volatile matter (i.e., 90.6%) that was detected, while the fixed carbon and ash were recorded at 6.07% and 3.33%, respectively.
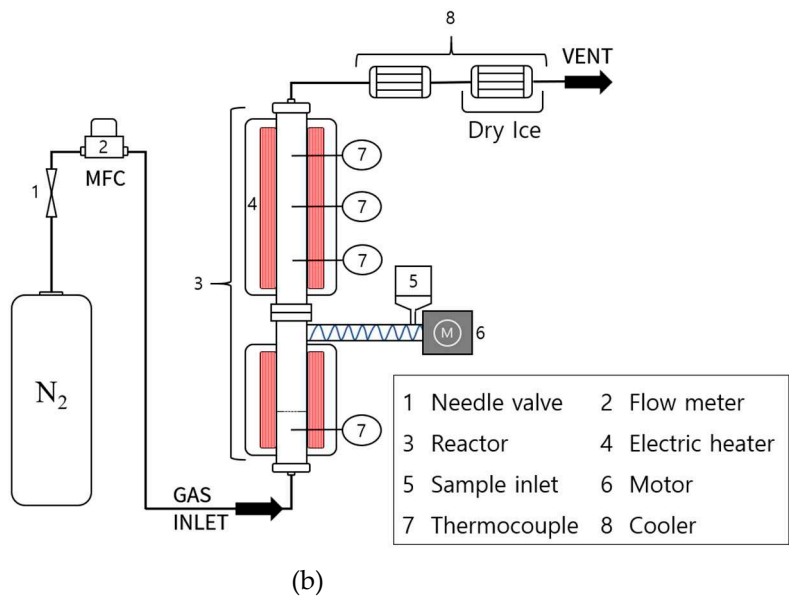
Table 2. Properties of SRF used in this work.

	C	63.1
	H	9.8
Elements (wt%)	N	0.6
	O	16.4
	S	0
	Other	10.1
Volatile (%)	90.60	
Fixed Carbon (%)	6.07	
Ash (%)	3.33	

3.2. Experimental Methods

The schematic diagrams of the fixed bed and fluidized bed reactors used in this study's pyrolysis experiments are shown in Figure 10. The fixed bed reactor (Figure 10a) consists of a quartz tube with a diameter and length of 60 and 550 mm, respectively. The pyrolysis products were collected through a two-stage cooler using cooling water and dry ice. For the fixed bed pyrolysis experiment, an initial 15g sample was loaded into a ceramic boat and inserted into the reactor. Heating was controlled by a PID controller until predetermined reaction temperatures of 550, 600, and 650℃ were reached. Nitrogen was introduced at a rate of 0.1L/min, and the experiment continued until the SRF was fully pyrolyzed. The resultant liquid recovered from the cooler and solid residues were then analyzed. The yield of gaseous products was calculated based on the initial sample weight and the amounts of liquid and solid residues. The fluidized bed reactor (Figure 10b) is designed to allow continuous sample injection, unlike the fixed bed reactor. It consists of a stainless steel tube, with a lower section that has a diameter and length of 62 and 370 mm, respectively, whereas its upper section has a diameter and length of 26 and 730 mm, respectively. Like the use of the fixed bed reactor, the pyrolysis products were collected through a two-stage cooler using cooling water and dry ice. In addition, 50g of sand with a diameter of 125-180 μm was used as the fluidizing medium for the fluidized bed reaction. The fluidized bed pyrolysis experiments were conducted at nitrogen flow rates ranging from 0.75 –1.5 L/min, allowing for optimal fluidization; these flow rates were adjusted at an interval of 0.25 L/min. Upon reaching the set reaction temperature, samples were continuously injected at a rate of 0.5-0.7g/min for one hour. Like in the case of the fixed bed reactor, pyrolysis was also set to occur at 550, 600, and 650℃, and these temperatures were controlled using a PID controller. Finally, yields of the liquid products were analyzed once products recovered from the cooler were collected. The amount of solid residue was analyzed by weighing the solid material remaining in the reactor and the initial sand used as the fluidizing medium after the experiment. The yield of gaseous products was calculated similarly to the fixed bed experiments, based on the initial SRF sample weight and the amounts of liquid and solid residues.

(a)

(b)

Figure 9. Schematic diagram of fixed (a) and fluidized (b) bed reactors used in this study.

The composition of the liquid products recovered through the fixed and fluidized bed reactors was analyzed using gas chromatography mass spectrometry (GC-MS) (GCMS-QP2010 Ultra, Dong-il SHIMADZU, Japan). The conditions under which the GC-MS was operated are presented in Table 3. Additionally, for the kinetic analysis of the pyrolysis reactions, thermal mass changes were analyzed using thermo gravimetric analysis (TGA) (Pyris 1 TGA, USA) at heating rates of 20, 30, and 40℃/min in a nitrogen atmosphere.

Table 3. Conditions under which the gas chromatography mass spectrometry (GC-MS) was used.

Item	Conditions
Column Over Temp	40.0℃
Injection Temp	250.0℃
Injection Mode	Split
Flow Control Mode	Linear Velocity
Pressure	60.1 kPa
Total Flow	234.1 mL/min
Column Flow(He)	1.15 mL/min
Linear Velocity	38.6 cm/sec
Purge Flow	3.0 mL/min
Split Ratio	200.0

3.3. Kinetic Analysis

The reaction rate equation for the conversion rate of pyrolysis can be represented by the following Arrhenius equation (1). Differential and integral approaches are widely used toward the kinetic analysis of a pyrolysis reaction using TGA results [23].

$$\frac{d\alpha}{dt} = Ae^{-\frac{E}{RT}}(1-\alpha)^n \tag{1}$$

where,　A : pre-exponential factor(min-1)

E : apparent activation energy(kJ/mol)

n : apparent order of reaction

R : gas constant(8.3136J/mol·K)

T : absolute temperature(K)

t : time(min)

α : degree of conversion

3.3.1. Differential Method

This method utilizes the following logarithmic differential equation derived from equation (1).

$$\ln\left(\frac{d\alpha}{dt}\right) = \ln\{A(1-\alpha)^n\} - \frac{E}{RT} \tag{2}$$

For fixed, the first term on the right-hand side of Equation (2) is constant. Therefore, plotting 1/T against α allows for the determination of the activation energy E from the slope.

3.3.2. Integral Method

By rearranging Equation (1) using the linear heating rate β (K/min), Equation (3) can be derived; Equation (3) can then be further rearranged to yield Equation (4).

$$\frac{d\alpha}{dT} = \frac{A}{\beta}e^{-\frac{E}{RT}}(1-\alpha)^n \tag{3}$$

$$\frac{d\alpha}{(1-\alpha)^n} = \frac{A}{\beta}e^{-\frac{E}{RT}}dT \tag{4}$$

Both sides of Equation (4) can be approximated through integration, as shown below [24]:

$$\int_0^\alpha \frac{d\alpha}{(1-\alpha)^n} \approx \frac{1-(1-\alpha)^n}{1-n} \qquad n \neq 1 \tag{5}$$

$$= -\ln(1-\alpha) \qquad n = 1 \tag{6}$$

and

$$A/\beta \int_0^T e^{-E/RT} dT \approx \frac{ART^2}{\beta E}(1 - \frac{2RT}{E})e^{-E/RT} \tag{7}$$

Additionally, taking the logarithm of Equations (5) to (7) yields Equations (8) and (9).

$$\ln\left\{\frac{1-(1-\alpha)^{1-n}}{T^2(1-n)}\right\} = \ln\frac{AR}{\beta E}\left(1 - \frac{2RT}{E}\right) - \frac{E}{RT} \qquad n \neq 1 \tag{8}$$

$$\ln\left\{\frac{-\ln(1-\alpha)^{1-n}}{T^2}\right\} = \ln\frac{AR}{\beta E}\left(1 - \frac{2RT}{E}\right) - \frac{E}{RT} \qquad n = 1 \tag{9}$$

Therefore, after assuming each reaction order, the activation energy values can be determined from the slopes of the plotted relations.

$$Y = -\ln\left\{\frac{1-(1-\alpha)^{1-n}}{T^2(1-n)}\right\} vs \frac{1}{T} \qquad n \neq 1 \tag{10}$$

$$Y = -\ln\left\{-\frac{\ln(1-\alpha)}{T^2}\right\} vs \frac{1}{T} \qquad n = 1 \tag{11}$$

Using Equations (10) and (11), the reaction orders n can be determined for the cases that best fit a straight line, and the activation energies can be obtained from the slopes of those lines.

4. Conclusions

We conducted a kinetic analysis study on the pyrolysis reaction of SRF made from plastic waste; the pyrolytic properties of the SRF were investigated using two reactors, namely, fixed bed and fluidized bed reactors. Based on the kinetic analysis of the pyrolytic reactions using differential and integral methods applied to the TGA results, we found that the activation energy is lower in the initial stage of pyrolysis, mainly due to the decomposition of PP components, compared to later stages in which PE decomposes. Using a fixed bed reactor, we found that as the reaction temperature increases, gasification becomes more vigorous, resulting in an increase and decrease in the yields of the gas and liquid, respectively. Via the fluidized bed reactor, we confirmed that, similar to the case of the fixed bed reactor, the gas yield increases as the reaction temperature increases and also rises as the flow rate of fluidizing gas increases. Overall, fluidized bed reactions result in a more active decomposition of SRF. The relatively superior performance of this reactor can be attributed to the increased material and heat transfer effects caused by fluidizing gases, which result in greater gas yields. Regarding the characteristics of liquid products generated during pyrolysis, fluidized bed reactions exhibited SRF decomposition more rapidly than that seen in the fixed bed reactor; compared to the outputs of the fixed bed reactor, these trends culminated in an increase in gas products and a corresponding

decrease in the hydrogen content in heavy oil, resulting in a higher C/H ratio and the production of heavier molecular components.

References

1. Horodyska, O.; Vakdes, F.J.; Fullana, A. Plastic flexible films waste management-A state of art review. *Waste Management* **2018**, *22*, 413-425.
2. Meys, R.; Frick, F.; Westhues, S.; Sternberg, A.; Klankermayer, J.; Bardow, A. Towards a circular economy for plastic packing waste-the environmental potential of chemical recycling. *Resources, Conservation & Recycling* **2020**, *162*, 105010.
3. Park, K.B.; Jeong, Y.S.; Guzelciftci, B.; Kim, J.S. Two-stage pyrolysis of polystyrene: Pyrolysis oil as a source of fuels or bezene, toluene, ethylbenzene, and xylene. *Applied Energy* **2020**, *259*, 114240.
4. Mangesh, V.L.; Padmanabhan, S.; Tamizhdural, P.; Ramesh, A. Experimental investigation to identify the type of waste plastic pyrolysis oil suitable for conversion to diesel engine fuel. *Journal of Cleaner Production* **2020**, *246*, 119066.
5. Sekar, M.; Ponnusamy, V.K.; Pugazhendhi, A.; Nizetic, S.; Praveenkumar, T.R. Production and utilization of pyrolysis oil from solid plastic wastes: A review on pyrolysis ptocess and influence of reactors design. *Journal of Environmental Management* **2022**, *302 Part B*, 114046.
6. Signh, R.K; Ruj, B.; Sadhukhan, A.K.; Gupta, P. Thermal degradation of waste plastics under non-sweeping atmosphere: Part 1 Effect of temperature, product optimization, and degradation mechanism. *Journal of Environmental Management* **2019**, *239*, 395-406.
7. Kunwar, B.; Cheng, H.N.; Chandrashekaran, S.R.; Sharma, B.K. Plastics to fuel: a review. *Renewable and Sustainable Energy Reviews* **2016**, *54*, 421-428.
8. Nimmegeers, P.; Billen, P. Quantifying the separation complexity of mixed plastic waste streams with statistical entropy: A plastic waste case study in Belgium. *ACS Sustainable Chemistry & Engineering* **2021**, *9*, 9813-9822.
9. Vollmer, I.; Jenks, M.J.F.; Roelands, M.C.P.; White, R.J.; van Harmelen, T.; de Wild, P., van der Laan, G.P.; Meirer, F.; Keurentjes, J.T.F.; Weckhuysen, B.M. Beyond mechanical recycling: Given new life to plastic waste, *Angewandte Chemie International Edition*, **2020**, *59*, 15402-15423.
10. Sharuddin, S.D.A.; Abnisa, F.; Daud, W.M.A.W.; Aroua, M.K. A review on pyrolysis of plastic wastes. *Energy Conservation and Management* **2016**, *115*, 308-326.
11. Jahirul, A.I.; Rasul, M.G.; Schaller, D.; Khan, M.M.K.; Hasan, M.M.; Hazrat, M.A. Transport fuel from waste plastics pyrolysis-A review on technologies challenges and opportunities. *Energy Conservation and Management* **2022**, *258*, 115451.
12. Qureshi, M.S.; Oasmaa, A.; Pihkola, H.; Deviatkin, I.; Tenhunen, A.; Mannila, J.; Minkkinen, H.; Pohjakallio, M.; Laine-Ylijoki, J. Pyrolysis of plastic waste: Opportunities and challenges. *Journal of Analytical and Applied Pyrolysis*. **2020**, 152, 104804.
13. Al-Salem. S.M.; Antelava, A.; Constantinou, A.; Manos, G.; Dutta, A. A review on thermal and catalytic pyrolysis of plastic solid waste (PSW). *Journal of Environmental Management* **2017**, *197*, 177-198.
14. Vellaiyan, S. Energy extraction from waste plastics and its optimization study for effective combustion and cleaner exhaust engaging with water and cetane improve: A response surface methodology approach. *Environmental Research* **2023**, *231 Part 1*, 116113.
15. Kaimal, V.K.; Vijayabalan, P. A detailed study of combustion characteristics of a DI diesel engine using waste plastic oil and its blends. *Energy Conservation and Management* **2015**, *105*, 951-956.

16. Wathakit, K.; Sukjit, E.; Kaewbuddee, C.; Maithomklang, S.; Klinkaew, N.; Liplap. P.; Arjharn, W.; Srisertpol, J. Characterization and impact of waste plastic oil in a bariable compression ration diesel engine. *Energies*, **2021**, *14*, 2230.

17. Panda, A.K.; Singh, R.K.; Mishra, D.K. Thermolysis of waste plastics to liquid fuel: A suitable method for plastic waste management and manufacture of value added products-A world prospective. *Renewable and Sustainable Energy Reviews* **2010**, *14*, 223-248.

18. Al-Salem, S.M.; Lettieri, P.; Baeyens, J. Recycling and recovery routes of plastic solid waste (PSW): A review. *Waste management* **2009**, *29*, 2625-2643.

19. Harussani, M.M.; Sapuan, S.M.; Rashid, U.; Khalina, A.; Ilyas, R.A. Pyrolysis of polypropylene plastic waste into carbonaceous char: Priority of plastic waste management amidst COVID-19 pandemic. *Science of the Total Environment* **2022**, *803*, 149911

20. Marcilla, A.; Garcia-Quesada, J.C.; Sanchez, S.; Ruiz, R. Study of the catalytic pyrolysis behaviour of polyethylene–polypropylene mixtures. *J. Anal. Appl. Pyrolysis* **2005**. *74*, 387–392.

21. Kim, H.T.; Oh, S.C. Kinetic of thermal degradation of waste polypropylene and high-density polyethylene. *J. Ind. Eng. Chem.* **2005**, *11*, 648-656.

22. Jung, S.-H.; Cho, M.-H.; Kang, B.-S.; Kim, J.-S. Pyrolysis of a fraction of waste polypropylene and polyethylene for the recovery of BTX aromatics using a fluidized bed reactor. *Fuel Process. Technol.* **2010**. *91*, 277–284.

23. Park, J.W,; Oh, S.C.; Lee, H.P.; Kim, H.T.; Yoo, K.O. Kinetic analysis of thermal decomposition of polymer using a dynamic model. *Korean J. Chem. Eng.* **2000**, *17*, 489-496.

24. Coats, A.; Redfern, J. Kinetic parameters from thermogravimetric data. *Nature*, **1964**, *201*, 68-69.